Collisional Loss of One-Dimensional Fermions Near a *p*-Wave Feshbach Resonance

Ya-Ting Chang, Ruwan Senaratne, Danyel Cavazos-Cavazos, and Randall G. Hulet*
Department of Physics and Astronomy, Rice University, Houston, Texas 77005, USA

(Received 4 July 2020; accepted 26 October 2020; published 30 December 2020)

We study collisional loss of a quasi-one-dimensional spin-polarized Fermi gas near a p-wave Feshbach resonance in ultracold ^{6}Li atoms. We measure the location of the p-wave resonance in quasi-1D and observe a confinement-induced shift and broadening. We find that the three-body loss coefficient L_3 as a function of the quasi-1D confinement has little dependence on confinement strength. We also analyze the atom loss with a two-step cascade three-body loss model in which weakly bound dimers are formed prior to their loss arising from atom-dimer collisions. Our data are consistent with this model. We also find a possible suppression in the rate of dimer relaxation with strong quasi-1D confinement. We discuss the implications of these measurements for observing p-wave pairing in quasi-1D.

DOI: 10.1103/PhysRevLett.125.263402

The realization of ultracold atomic Fermi gases has provided experimental access to a wide array of phenomena, largely because of the presence of Feshbach resonances (FRs) that provide for externally tunable interactions [1–4]. In addition to the usual s-wave interactions between distinguishable fermions, higher partial-wave interactions may be tuned via FRs [5]. p-wave interactions are of particular interest as they are the dominant low-energy scattering process between identical fermions and are predicted to exhibit phenomena distinct from those observed in s-wave interacting Fermi gases [6]. In particular, pairing between identical fermions is an essential ingredient of the Kitaev chain Hamiltonian [7], which supports Majorana zero modes at the ends of the chain. These zero modes have been observed in semiconducting nanowires [8] and are a promising candidate platform for fault-tolerant quantum computing [9,10].

p-wave FRs have been observed in ^{40}K [11–13] and ^{6}Li [14–19]. The severe atom losses associated with these resonances, however, have limited their usefulness. Three-body losses, which are suppressed by symmetry in the case of a fermionic two-spin system with s-wave interactions [20], are not suppressed for p-wave interactions. Much work has been done in characterizing the atom loss associated with p-wave FRs [21–24], and there is renewed interest in studying these resonances in reduced dimensions. Recent theoretical work has suggested that three-body losses may be suppressed in quasi-1D [25]. The absence of a centrifugal barrier in 1D results in Feshbach dimers that have extended wave functions which overlap less with deeply bound molecules. If three-body loss is suppressed by this mechanism, it might open a path toward realizing p-wave pairing in quasi-1D and emulating the Kitaev chain Hamiltonian.

We present an experimental study of three-body losses near a p-wave FR of identical ^{6}Li fermions in quasi-1D. We measure the three-body loss coefficient (L_3) as a function of 1D confinement for a direct three-body process. We also analyze the observed atom loss within the framework of a cascade model with explicit dimer formation and relaxation steps [26,27], using *in situ* imaging to reduce the effect of the inhomogeneous density. Finally, we characterize the confinement-induced shifts in the resonance position that appear in quasi-1D [28–32]. These shifts allow us to extract a value for the effective range.

The apparatus and the experimental methods we use to prepare degenerate Fermi gases have been described previously [33–35]. A ^{6}Li degenerate Fermi gas is first prepared in the two lowest hyperfine states of the $S_{1/2}$ manifold (states $|1\rangle$ and $|2\rangle$, respectively) at 595 G, and then loaded into a crossed-beam dipole trap formed by three linearly polarized mutually orthogonal laser beams of wavelength $\lambda = 1.064\ \mu$m. Each beam is retroreflected, with the polarizations of the incoming and retroreflected beams initially set to be perpendicular to each other to avoid lattice formation. We eliminate state $|1\rangle$ from the trap with a resonant burst of light. At this stage, we obtain $9(1) \times 10^4$ atoms in state $|2\rangle$ in a nearly isotropic harmonic trap with a geometric-mean trapping frequency of $2\pi \times 305(2)$ Hz, and at a temperature $T/T_F \approx 0.1$ where T_F is the Fermi temperature. The optical trap depths are increased and the polarizations of the retroreflected beams are rotated to achieve a 7 E_r deep 3D optical lattice, where $E_r = h^2/(2m\lambda^2) = k_B \times 1.41\ \mu$K is the recoil energy, and m is the atomic mass. During the lattice ramp-up, a copropagating beam of 532 nm light is introduced along each trapping-beam dimension to flatten the trapping potential [33,34]. By tuning these compensation beam powers, we create a 3D band insulator with a central density of approximately 1 atom per site. In order to produce a 2D lattice, which is an array of quasi-1D tubes, we slowly turn off the compensation beams and the vertical lattice beam, while increasing the intensity of the two remaining beams to achieve a desired 2D lattice depth V_L. This depth determines the confinement in the quasi-1D traps, which is parametrized by $a_\perp = \sqrt{2\hbar/m\omega_r}$ transversely and R_F axially, where $\omega_r = \sqrt{4E_r V_L}/\hbar$ is the trapping frequency of a lattice site when approximated as a harmonic potential, and $R_F(N_{t,j},\omega_z) = \sqrt{(2N_{t,j}+1)\hbar/m\omega_z}$ is the Fermi radius of tube j with number of atoms $N_{t,j}$ and an axial frequency ω_z. The aspect ratio of the quasi-1D tubes $\omega_r/\omega_z \approx 170$. We load a maximum of around 30 atoms per quasi-1D tube with $T < T_F$ to avoid exciting any radial modes.

We use a two-step servo scheme to stabilize the current in the coils producing the Feshbach magnetic field, because the ^{6}Li $|1\rangle - |1\rangle$ p-wave FR near 159 G is very narrow. The first servo S_1 provides the large dynamic range required to run our experimental sequence, while the second servo S_2 controls the current in a bypass circuit added in parallel to the magnetic coils. This improves the stability of the magnetic field to ± 10 mG and provides finer magnetic-field resolution. After reaching the hold field B, the atoms are transferred into $|1\rangle$ with a π pulse of duration 75 μs using rf radiation resonant with the $|1\rangle - |2\rangle$ transition. After a hold time τ, we ramp the field back to 595 G, where the distribution of the remaining atoms is imaged using *in situ* phase-contrast imaging with a probe beam propagating perpendicular to the tube axis [35]. By using the inverse Abel transform, which exploits the approximate cylindrical symmetry of the 2D lattice, we measure the distribution with a spatial resolution of approximately three lattice constants. We sector the 2D lattice into concentric shells in which the tubes have similar chemical potentials μ. This procedure is useful as scattering processes are in general energy dependent, so observables depend on rate coefficients that are averaged over the Fermi-Dirac distribution for atoms in each tube.

We characterize the $|1\rangle - |1\rangle$ p-wave FR in 3D and quasi-1D by measuring atom loss as functions of B and τ. In 3D, we find the onset of loss at 159.05(1) G, which agrees with previous measurements of the location of this resonance in 3D [15,17] but differs with other measurements [19,36] by a few tens of milligauss. We are not able to resolve the expected doublet feature arising from the dipole-dipole interaction [12,19,37] because of limitations of the field stability. All the 1D data in this Letter were measured with the magnetic field aligned with the z axis, and thus only involve collisions with the $m_l = 0$ projection of the angular momentum. As V_L is increased, we observe a confinement-induced shift in the resonance field and broadening of the atom-loss feature, as shown in Fig. 1(a).

We review p-wave scattering in 3D and quasi-1D to show how the measured confinement-induced shift can be used to extract α_p, the 3D effective range. For low-energy collisions in 3D, the cotangent of the phase shift δ_p associated with

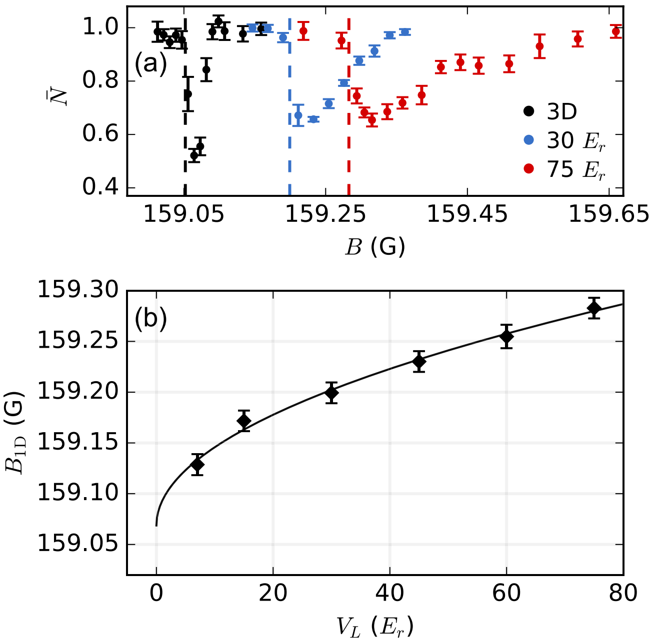

FIG. 1. (a) p-wave resonances in 3D and quasi-1D measured with magnetic-field-dependent loss. Dashed lines show the resonance position for each V_L. We define the resonance field for zero-momentum collisions, which corresponds to the onset (15% loss, to overcome atom number fluctuation) of the observed atomic loss. Data are averaged over 6 experimental runs and error bars are the standard error of the mean. (b) Diamonds show B_{1D} versus V_L. The solid curve shows the result of fitting the data to Eq. (3), where the effective range $\alpha_p = 0.14(1)a_0^{-1}$ and $B_{3D} = 159.07(1)$ G are fitted parameters. Error bars are the statistical uncertainty arising from atom number fluctuation and field instability. In both (a) and (b), τ is chosen such that peak loss is 30%–50% of total atom number for each value of V_L: 2.5 ms for 3D, 0.5 ms for $7E_r$, and 0.2 ms for 15–75 E_r.

p-wave scattering can be expanded as a function of scattering volume V_p and effective range α_p [38]:

$$k^3 \cot[\delta_p(k)] = -\frac{1}{V_p} - \alpha_p k^2 + O(k^4), \tag{1}$$

where $\alpha_p > 0$ and has units of inverse length. These scattering properties are modified in quasi-1D,

$$k \cot[\delta_p(k)] = -\frac{1}{l_p} - \xi_p k^2 + O(k^4), \tag{2}$$

where l_p is the 1D scattering length and ξ_p is the 1D effective range, which has units of length. These quasi-1D scattering parameters are given by $l_p = 3a_\perp[a_\perp^3/2V_p + \alpha_p a_\perp + 6|\zeta(-1/2)|]^{-1}$ and $\xi_p = \alpha_p a_\perp^2/6$ [30–32], where ζ is the Riemann zeta function [$\zeta(-1/2) \approx -0.208$]. The second and third terms in $1/l_p$ lead to a confinement-induced shift in the resonance location. In this formalism, only dynamics along the axial dimension are relevant, and scattering quantities, such as the elastic scattering cross section, are expressed in units appropriate for 1D.

By performing a coupled-channel calculation, which requires detailed knowledge of the interatomic potentials [39], we obtain an expansion $1/V_p(B)$ up to second order in B. The effective range α_p can be approximated as a constant independent of B for the relevant range of magnetic field. The FR in 3D occurs at the magnetic field $B_{3\mathrm{D}}$ at which V_p diverges. Similarly, in quasi-1D, the resonance occurs when l_p diverges at a magnetic field $B_{1\mathrm{D}}$, which is a function of V_L and α_p. The confinement-induced shift, $\delta_B(V_L, \alpha_p) = B_{1\mathrm{D}} - B_{3\mathrm{D}}$, can be approximated to leading order in confinement strength V_L by [40]

$$\delta_B = \frac{-2m}{\hbar^2 \frac{\partial(1/V_p)}{\partial B}\big|_{B=B_{3D}}} \alpha_p \sqrt{V_L E_r} \tag{3}$$

We cannot accurately measure $B_{3\mathrm{D}}$ for $m_l = 0$ alone due to the unresolved $|m_l| = 1$ collisions in 3D, so we fit the measured δ_B as a function of V_L to Eq. (3) by taking α_p and $B_{3\mathrm{D}}$ as fitting parameters. The result of the fit to the quasi-1D data is shown by the solid curve in Fig. 1(b). We obtain $\alpha_p = 0.14(1)a_0^{-1}$ which is consistent with our coupled-channel result of $0.1412a_0^{-1}$, where a_0 is the Bohr radius, and $B_{3\mathrm{D}} = 159.07(1)$ which is consistent with our loss-onset measurement and a dipolar splitting of 10 mG in 3D [19]. We also find a consistent value by analyzing previous measurements performed on a 2D gas of ^{6}Li in state $|1\rangle$ [21,40].

The observed atom loss is presumably due to the formation of deeply bound molecules. To characterize the loss, we measured N, the number of atoms remaining in the trap after a hold time τ, for various B and V_L. Background-gas collisions lead to a $1/e$ atom lifetime of 38 s in this apparatus, and are negligible for this analysis. Atom loss due to three-body collisions is described by

$$\frac{\dot{N}}{N} = -L_3 n^2, \tag{4}$$

where $n^2 = (N_{t,c}/2R_{F,c})^2$ is the squared atomic line density for a central tube, determined using a length scale of twice the local Fermi radius $R_{F,c}$. We measure the time evolution with V_L between 15 and 75 E_r and extract L_3 by fitting loss versus τ to Eq. (4). Figure 2(a) shows such a fit to typical loss data. Since L_3 also depends on ΔB, the field detuning from resonance, we extract L_3 from the time evolution at several ΔB to find the peak value for each V_L. The peak L_3 for all V_L are found to be approximately $7(2) \times 10^{-6}$ cm^2/s. We observe no dependence on 1D confinement in this range [40]. Because of the inhomogeneity of the initial distribution of atoms across the 2D lattice, however, we find a rather poor agreement of the data to Eq. (4).

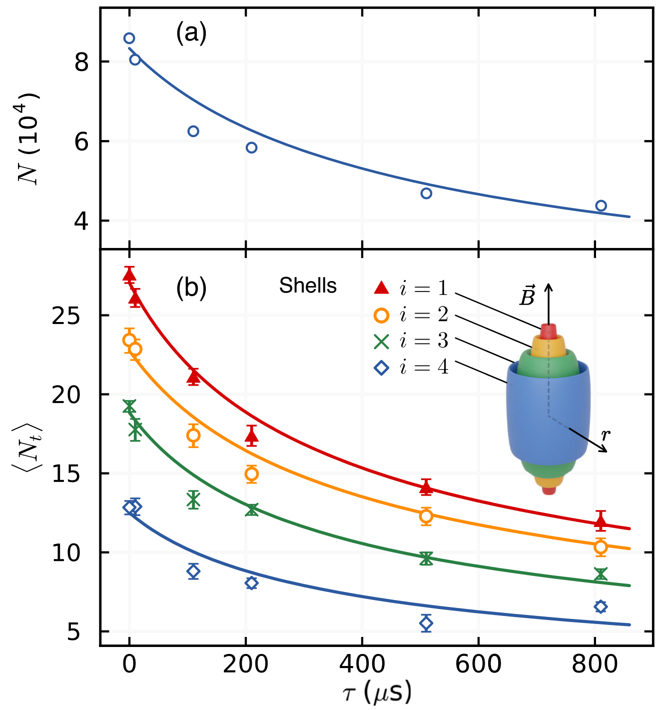

FIG. 2. Typical time evolution of (a) total number in the entire sample and (b) the average tube population $\langle N_t \rangle$ in each of 4 shells. For these data, $\Delta B = 30$ mG and $V_L = 75\ E_r$. The different colors and symbols in (b) indicate different shells with approximately uniform initial atom number per tube. The shells are labeled from $i = 1$, the innermost, to $i = 4$, the outermost. Solid curves show fits to the direct three-body loss model expressed by Eq. (4) to extract L_3 with the squared atomic density (a) $n^2 = (N_{t,c}/2R_{F,c})^2$ of a central tube and (b) $n^2 = (\langle N_t \rangle_i / 2R_{F,i})^2$ of a typical tube in each shell. The corresponding L_3 values are plotted in Fig. 3. Data points are averaged over 5 shots, and the standard error of the mean is (a) approximately equal to the symbol size and (b) indicated by the error bars.

The results of a more comprehensive analysis of the same data that provides an improved fit to Eq. (4) is shown in Fig. 2(b). Here, we group the tubes into separate cylindrical shells (labeled by $i = 1$–4) with an average atom number per tube $\langle N_t \rangle_i$ [40] and a corresponding Fermi temperature $T_{F,i}$. Since the tunneling rate is small compared to the hold time, we assume that the atoms remain in the same tube, and thus the same shell during the collision process. Figure 3(a) shows L_3 for each shell extracted from data with $V_L = 75\ E_r$ versus ΔB. The peak L_3 for each shell is in the range of 5×10^{-6} to 1×10^{-5} cm^2/s, and is similar to the peak L_3 extracted from the whole atomic cloud.

In Ref. [25], Zhou and Cui suggest that the rate of three-body loss near a p-wave FR can be suppressed by reducing the overlap between the wave functions of a deeply bound molecule and a Feshbach dimer with increasing confinement. To investigate this hypothesis, we analyze our observed loss data using a cascade model of two consecutive two-body processes instead of a direct three-body event: two atoms resonantly form a dimer, followed by a collision between the dimer and an atom, resulting in a deeply bound molecule and an atom [26]. This approach has previously been applied to the particular p-wave FR we study, but in 3D and quasi-2D [27]. It is the natural formalism in which to evaluate the predicted suppression, as it models the formation and relaxation of dimers. The equations governing this loss process are

$$\frac{dN_a}{dt} = 2\frac{\Gamma}{\hbar}N_d - 2K_{aa}\frac{N_a(N_a-1)}{4R_F} - K_{ad}\frac{N_aN_d}{2R_F}, \quad (5a)$$

$$\frac{dN_d}{dt} = -\frac{\Gamma}{\hbar}N_d + K_{aa}\frac{N_a(N_a-1)}{4R_F} - K_{ad}\frac{N_aN_d}{2R_F}, \quad (5b)$$

where N_a is the number of atoms, N_d is the number of dimers, K_{aa} is the two-body event rate for atom-atom collisions converting atoms into dimers, and K_{ad} is the two-body atom-dimer inelastic collision event rate. Γ, the one-body decay rate of dimers, is the width of the FR. The rate of dimer formation is proportional to the number of possible pairs of atoms, given by $N_a(N_a-1)/2!$.

K_{ad} is of particular interest, as it depends on the overlap between dimers and deeply bound molecules. Both Γ and K_{aa} are related to the elastic scattering cross section $\sigma_{1\mathrm{D}}(E)$, which can be calculated, thus constraining the fit to the cascade process to a single parameter, K_{ad}. $\sigma_{1\mathrm{D}}(E)$ may be approximated by a Lorentzian in collision energy, $E = \hbar^2k^2/m$, centered at the above-threshold binding energy of the Feshbach dimer $E_{\mathrm{res}} = -\hbar^2/l_p\xi_p m > 0$ and with width $\Gamma = (\hbar/\xi_p)\sqrt{4E_{\mathrm{res}}/m}$ [6,40].

K_{aa} may be calculated by averaging $\sigma_{1\mathrm{D}}(k_r)$ over the ensemble of pairs of atoms with relative momentum k_r and velocity v_r,

$$K_{aa} = \langle\sigma_{1\mathrm{D}}(k_r)v_r\rangle = \hbar\int_{-\infty}^{\infty} dk_r\sigma_{1\mathrm{D}}(k_r)v_rP(k_r), \quad (6)$$

where $P(k_r)$ is the probability density function of k_r obtained from the density distribution of a trapped Fermi gas [40]. We assume a global temperature T across the entire sample. However, μ varies significantly from tube to tube due to the density inhomogeneity across the 2D lattice. This effect is mitigated by sectoring the cloud into shells of similar μ, as discussed earlier, thus giving a distinct value of K_{aa} for each shell. For each quasi-1D tube, μ is determined by $N_{t,j}$ and T.

Although we cannot directly measure T, we exploit the fact that at a sufficiently large ΔB, the rate equations can be approximated as a direct three-body loss process with a loss coefficient $\tilde{L}_3 = (3/2)\hbar K_{ad}K_{aa}/\Gamma$ under the assumptions of a steady-state dimer population $(dN_d/dt = 0)$ and $\Gamma/\hbar \gg K_{ad}N_a/2R_F$ [27]. Assuming that these assumptions hold for large ΔB, we fit the measured values of L_3 for each shell with T and K_{ad} as fitting parameters to $\tilde{L}_3$. We find that $T = 0.1T_{F,1}$, and that $K_{ad} = 0.67$ cm/s is independent of field for $\Delta B > 100$ mG. The assumptions given above are confirmed in this range. The solid lines in Fig. 3(a) show $\tilde{L}_3$ for each shell.

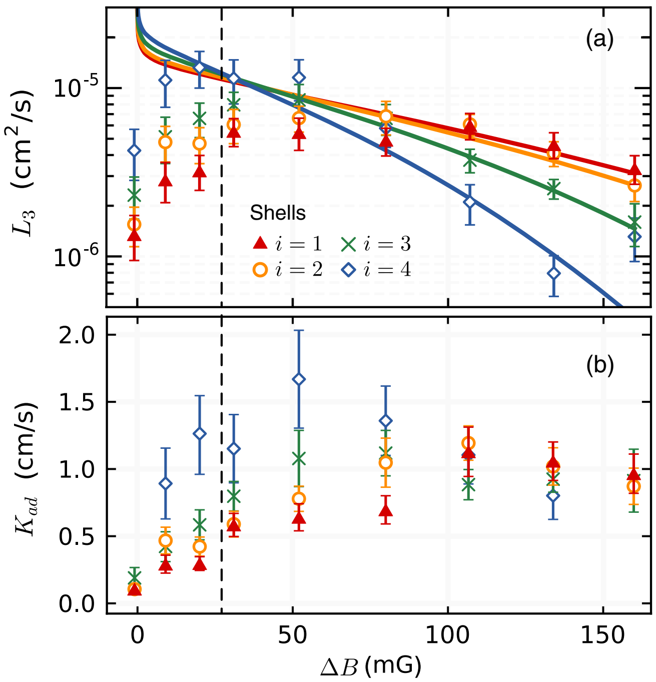

FIG. 3. (a) L_3 versus ΔB for $V_L = 75\ E_r$. L_3 is obtained by fitting $N_{t,i}$ versus τ to Eq. (4) for each shell. An example of these data is given in Fig. 2(b) for $\Delta B = 30$ mG. Solid curves show $(3/2)\hbar K_{ad}K_{aa}/\Gamma$ with a constant $K_{ad} = 0.67$ cm/s, calculated for $T = 0.1T_{F,1}$, where $T_{F,1} = 4.8(2)\ \mu$K. (b) K_{ad} versus ΔB. K_{ad} is extracted by fitting $\langle N_t\rangle_i$ versus τ to Eqs. (5), using the calculated values of Γ and K_{aa}. Black dashed line indicates $\Delta B = 27$ mG, which corresponds to $\kappa a_\perp = 1/2$ for $V_L = 75\ E_r$ [25]. Error bars are 1σ confidence intervals for the fitting parameters L_3 and K_{ad}. The large uncertainty in the fitted values for the outermost shell is indicative of small N_t.

The extracted K_{ad} values from fitting loss data for $V_L = 75\ E_r$ to Eqs. (5) using the calculated values of Γ and K_{aa} are shown in Fig. 3(b) for the full range of ΔB [40]. We find that under these conditions, Eqs. (5) model the time behavior of the observed loss as well as Eq. (4), as there is little difference between the fit to the cascade model [40] and the direct three-body loss model. The values of K_{ad} extracted for $\Delta B > 50$ mG are field independent. The observed field independence strongly supports the cascade model as the atom-dimer collision process is inherently nonresonant. In the dimer formation step, the atoms must collide with a momentum dictated by the binding energy of the dimer, which is field dependent. The dimer relaxation step, however, may proceed for any collision momentum, as the atom receives the binding energy of the deeply bound molecule.

The behavior of K_{ad} for $\Delta B < 50$ mG is consistent with a suppression of the rate of dimer relaxation. The spatial overlap of the dimer and deeply bound wave functions increases with $\kappa a_\perp$, where $\kappa = \sqrt{mE_{\mathrm{res}}}/\hbar$, so the predicted suppression is strongest for small ΔB, where E_{res} is smallest. The suppression is expected to be significant for $\kappa a_\perp < 1/2$ [25], which for $V_L = 75\ E_r$ corresponds to $\Delta B < 27$ mG. Another interpretation of the small-detuning behavior of K_{ad} is that the cascade model breaks down due to, for example, the existence of a shallow three-body bound state [41].

This work is the first detailed experimental study of p-wave collisions in quasi-1D. We confirm the confinement-induced shift and broadening as a function of V_L. The confinement-induced shift agrees well with quasi-1D theory [32] and the extracted value of α_p agrees with previous work [21]. We measure L_3 as a function of V_L and find no dependence up to 75 E_r. The magnetic field independence of K_{ad} for $\Delta B > 50$ mG strongly supports the validity of the cascade model [26,27] for three-body loss in quasi-1D in the regime of large ΔB (> 100 mG), as well as for intermediate ΔB (50–100 mG) where the cascade model is not well approximated by the three-body loss rate equation.

The suppression in K_{ad} at $\Delta B < 50$ mG is possibly explained by p-wave dimer stretching [25]. Achieving greater suppression in ^{6}Li by increasing V_L is challenging since at a fixed ΔB, $\kappa a_\perp \propto 1/V_L^{1/4}$ [40], but future work at even higher V_L or with improved magnetic field resolution and stability would enable further study of this narrow feature. The implications for loss suppression due to the closed-channel character of the p-wave resonance used here remains to be fully understood theoretically. Our result also provides insight into a potential pathway toward observing pairing between identical fermions in cold atom systems. Suppressing loss in heavier fermions with FRs, such as ^{40}K [11–13], ^{161}Dy [42], and ^{167}Er [43], is promising, as small values of $\kappa a_\perp$ may be more readily achieved in these atoms.

We would like to thank T. L. Yang for his contributions to the apparatus and W. I. McAlexander for his coupled-channel code. This work was supported in part by the Army Research Office Multidisciplinary University Research Initiative (Grants No. W911NF-14-1-0003 and No. W911NF-17-1- 0323), the NSF (Grant No. PHY-1707992), and the Welch Foundation (Grant No. C-1133). D. C.-C. acknowledges financial support from CONACyT (Mexico, Scholarship No. 472271).

Note added.—Recently, another group reported on a similar experiment [44]. Although both groups observe similar overall atom loss, they report a suppression of $L_3 \propto V_L^{-1}$, while we find L_3 independent of V_L over a wide range (Fig. S2 of Supplemental Material [40]). The difference lies in the choice between defining L_3 using the 3D or the 1D densities. In their analysis, L_3 is defined in terms of the 3D density of a tube, which increases with $V_L^{1/2}$, while we use the 1D line density. While the two results are consistent, we argue that 1D densities are most appropriate based on physical and practical considerations. Physically, the dimensionless quantity $\kappa a_\perp$ parametrizes the effective dimensionality of the system near a FR, and the peak values of L_3 we report were measured in regions where $\kappa a_\perp < 1$. Practically, 1D units make it clear that the peak loss rate is independent of V_L.

*Corresponding author.
randy@rice.edu

[1] B. DeMarco and D. S. Jin, Onset of Fermi degeneracy in a trapped atomic gas, Science **285**, 1703 (1999).
[2] A. G. Truscott, K. E. Strecker, W. I. McAlexander, G. B. Partridge, and R. G. Hulet, Observation of Fermi pressure in a gas of trapped atoms, Science **291**, 2570 (2001).
[3] F. Schreck, L. Khaykovich, K. L. Corwin, G. Ferrari, T. Bourdel, J. Cubizolles, and C. Salomon, Quasipure Bose-Einstein Condensate Immersed in a Fermi Sea, Phys. Rev. Lett. **87**, 080403 (2001).
[4] S. R. Granade, M. E. Gehm, K. M. O'Hara, and J. E. Thomas, All-Optical Production of a Degenerate Fermi Gas, Phys. Rev. Lett. **88**, 120405 (2002).
[5] C. Chin, R. Grimm, P. Julienne, and E. Tiesinga, Feshbach resonances in ultracold gases, Rev. Mod. Phys. **82**, 1225 (2010).
[6] V. Gurarie and L. Radzihovsky, Resonantly paired fermionic superfluids, Ann. Phys. (Amsterdam) **322**, 2 (2007).
[7] A. Y. Kitaev, Unpaired Majorana fermions in quantum wires, Phys. Usp. **44**, 131 (2001).
[8] S. D. Sarma, M. Freedman, and C. Nayak, Majorana zero modes and topological quantum computation, Quantum Inf. **1**, 15001 (2015).
[9] S. B. Bravyi and A. Y. Kitaev, Fermionic quantum computation, Ann. Phys. (Amsterdam) **298**, 210 (2002).
[10] A. Stern and N. H. Lindner, Topological quantum computation—from basic concepts to first experiments, Science **339**, 1179 (2013).
[11] C. A. Regal, C. Ticknor, J. L. Bohn, and D. S. Jin, Tuning p-Wave Interactions in an Ultracold Fermi Gas of Atoms, Phys. Rev. Lett. **90**, 053201 (2003).
[12] K. Günter, T. Stöferle, H. Moritz, M. Köhl, and T. Esslinger, p-Wave Interactions in Low-Dimensional Fermionic Gases, Phys. Rev. Lett. **95**, 230401 (2005).
[13] C. Luciuk, S. Trotzky, S. Smale, Z. Yu, S. Zhang, and J. H. Thywissen, Evidence for universal relations describing a gas with p-wave interactions, Nat. Phys. **12**, 599 (2016).
[14] J. Zhang, E. G. M. van Kempen, T. Bourdel, L. Khaykovich, J. Cubizolles, F. Chevy, M. Teichmann, L. Tarruell, S. J. J. M. F. Kokkelmans, and C. Salomon, P-wave Feshbach resonances of ultracold ^{6}Li, Phys. Rev. A **70**, 030702 (2004).
[15] C. H. Schunck, M. W. Zwierlein, C. A. Stan, S. M. F. Raupach, W. Ketterle, A. Simoni, E. Tiesinga, C. J. Williams, and P. S.

Julienne, Feshbach resonances in fermionic ^{6}Li, Phys. Rev. A **71**, 045601 (2005).
[16] Y. Inada, M. Horikoshi, S. Nakajima, M. Kuwata-Gonokami, M. Ueda, and T. Mukaiyama, Collisional Properties of p-Wave Feshbach Molecules, Phys. Rev. Lett. **101**, 100401 (2008).
[17] J. Fuchs, C. Ticknor, P. Dyke, G. Veeravalli, E. Kuhnle, W. Rowlands, P. Hannaford, and C. J. Vale, Binding energies of ^{6}Li p-wave Feshbach molecules, Phys. Rev. A **77**, 053616 (2008).
[18] R. A. W. Maier, C. Marzok, C. Zimmermann, and P. W. Courteille, Radio-frequency spectroscopy of ^{6}Li p-wave molecules: Towards photoemission spectroscopy of a p-wave superfluid, Phys. Rev. A **81**, 064701 (2010).
[19] M. Gerken, B. Tran, S. Häfner, E. Tiemann, B. Zhu, and M. Weidemüller, Observation of dipolar splittings in high-resolution atom-loss spectroscopy of ^{6}Li p-wave Feshbach resonances, Phys. Rev. A **100**, 050701 (2019).
[20] D. S. Petrov, C. Salomon, and G. V. Shlyapnikov, Weakly Bound Dimers of Fermionic Atoms, Phys. Rev. Lett. **93**, 090404 (2004).
[21] M. Waseem, Z. Zhang, J. Yoshida, K. Hattori, T. Saito, and T. Mukaiyama, Creation of p-wave Feshbach molecules in selected angular momentum states using an optical lattice, J. Phys. B **49**, 204001 (2016).
[22] M. Waseem, T. Saito, J. Yoshida, and T. Mukaiyama, Two-body relaxation in a Fermi gas at a p-wave Feshbach resonance, Phys. Rev. A **96**, 062704 (2017).
[23] J. Yoshida, T. Saito, M. Waseem, K. Hattori, and T. Mukaiyama, Scaling Law for Three-Body Collisions of Identical Fermions with p-Wave Interactions, Phys. Rev. Lett. **120**, 133401 (2018).
[24] M. Waseem, J. Yoshida, T. Saito, and T. Mukaiyama, Unitarity-limited behavior of three-body collisions in a p-wave interacting Fermi gas, Phys. Rev. A **98**, 020702 (2018).
[25] L. Zhou and X. Cui, Stretching p-wave molecules by transverse confinements, Phys. Rev. A **96**, 030701 (2017).
[26] J. Li, J. Liu, L. Luo, and B. Gao, Three-Body Recombination near a Narrow Feshbach Resonance in ^{6}Li, Phys. Rev. Lett. **120**, 193402 (2018).
[27] M. Waseem, J. Yoshida, T. Saito, and T. Mukaiyama, Quantitative analysis of p-wave three-body losses via a cascade process, Phys. Rev. A **99**, 052704 (2019).
[28] M. Olshanii, Atomic Scattering in the Presence of an External Confinement and a Gas of Impenetrable Bosons, Phys. Rev. Lett. **81**, 938 (1998).
[29] T. Bergeman, M. G. Moore, and M. Olshanii, Atom-Atom Scattering under Cylindrical Harmonic Confinement: Numerical and Analytic Studies of the Confinement Induced Resonance, Phys. Rev. Lett. **91**, 163201 (2003).
[30] B. E. Granger and D. Blume, Tuning the Interactions of Spin-Polarized Fermions Using Quasi-One-Dimensional Confinement, Phys. Rev. Lett. **92**, 133202 (2004).
[31] L. Pricoupenko, Resonant Scattering of Ultracold Atoms in Low Dimensions, Phys. Rev. Lett. **100**, 170404 (2008).
[32] D. V. Kurlov and G. V. Shlyapnikov, Two-body relaxation of spin-polarized fermions in reduced dimensionalities near a p-wave Feshbach resonance, Phys. Rev. A **95**, 032710 (2017).
[33] R. A. Hart, P. M. Duarte, T.-L. Yang, X. Liu, T. Paiva, E. Khatami, R. T. Scalettar, N. Trivedi, D. A. Huse, and R. G. Hulet, Observation of antiferromagnetic correlations in the Hubbard model with ultracold atoms, Nature (London) **519**, 211 (2015).
[34] T. L. Yang, P. Grišins, Y. T. Chang, Z. H. Zhao, C. Y. Shih, T. Giamarchi, and R. G. Hulet, Measurement of the Dynamical Structure Factor of a 1D Interacting Fermi Gas, Phys. Rev. Lett. **121**, 103001 (2018).
[35] R. G. Hulet, J. H. V. Nguyen, and R. Senaratne, Methods for preparing quantum gases of lithium, Rev. Sci. Instrum. **91**, 011101 (2020).
[36] T. Nakasuji, J. Yoshida, and T. Mukaiyama, Experimental determination of p-wave scattering parameters in ultracold ^{6}Li atoms, Phys. Rev. A **88**, 012710 (2013).
[37] C. Ticknor, C. A. Regal, D. S. Jin, and J. L. Bohn, Multiplet structure of Feshbach resonances in nonzero partial waves, Phys. Rev. A **69**, 042712 (2004).
[38] C. J. Joachain, *Quantum Collision Theory* (North-Holland, Amsterdam, 1975).
[39] M. Houbiers, H. T. C. Stoof, W. I. McAlexander, and R. G. Hulet, Elastic and inelastic collisions of ^{6}Li atoms in magnetic and optical traps, Phys. Rev. A **57**, R1497 (1998).
[40] See Supplemental Material at http://link.aps.org/supplemental/10.1103/PhysRevLett.125.263402 for information regarding the derivation of Eq. (3), the confinement-induced shift in quasi-2D, the dependence of L_3 versus V_L, in situ imaging data, the fitting of time evolution data to the cascade model, the quasi-1D p-wave scattering cross section, the probability density function of k_r, and the dependence of $\kappa a_\perp$ on V_L.
[41] M. Schmidt, H.-W. Hammer, and L. Platter, Three-body losses of a polarized Fermi gas near a p-wave Feshbach resonance in effective field theory, Phys. Rev. A **101**, 062702 (2020).
[42] K. Baumann, N. Q. Burdick, M. Lu, and B. L. Lev, Observation of low-field Fano-Feshbach resonances in ultracold gases of dysprosium, Phys. Rev. A **89**, 020701 (2014).
[43] S. Baier, D. Petter, J. H. Becher, A. Patscheider, G. Natale, L. Chomaz, M. J. Mark, and F. Ferlaino, Realization of a Strongly Interacting Fermi Gas of Dipolar Atoms, Phys. Rev. Lett. **121**, 093602 (2018).
[44] A. S. Marcum, F. R. Fonta, A. M. Ismail, and K. M. O'Hara, Suppression of Three-Body Loss Near a p-Wave Resonance due to Quasi-1D Confinement, arXiv:2007.15783 [Phys. Rev. Lett. (to be published)].